*Int. J. Morphol.*,
*44(3)*:959-967, 2026.

http://dx.doi.org/10.4067/s0717-95022026000300959

# Evaluation of the Golden Ratio in Atlas with its Unique Anatomical Features

## Evaluación de la Proporción Áurea en el Atlas y sus Características Anatómicas Únicas

**Seda Sertel Meyvaci[1]; Handan Ankarali[2]; Duygu Goller Bulut[3]; Beyza Celik[1] & Betul Taskin[4]**

**SERTEL MEYVACI, S.; ANKARALI, H.; GOLLER BULUT, D.; CELIK, B. & TASKIN, B.** Evaluation of the golden ratio in atlas with its unique anatomical features. *Int. J. Morphol., 44(3)*:959-967, 2026.

**SUMMARY:** This study aimed to evaluate whether selected morphometric ratios of the atlas conform to the golden ratio by analyzing anatomical landmarks and parameters specific to its unique morphology. Cone beam computed tomography images of 359 individuals (180 males, 179 females), aged 18–82 years, were analyzed to assess the morphometric parameters of the atlas. 22 morphometric parameters of the atlas were measured, and 57 ratios were calculated from these measurements. Based on the mean value of each assessed ratio and the corresponding standard deviation (SD), the cases were classified into four groups. Descriptive statistics of the measurements and calculated ratios were determined, including mean, SD, median, 25th and 75th percentiles, count, and percentage frequencies. The deviation of the calculated ratios from the golden ratio was examined using a One-Sample t-test. Among the 57 calculated ratios, the golden ratio was observed only in P9/P22 ($p = 0.410$) and P18/P14 ($p = 0.159$). Several other ratios had mean values close to 1.618, including P1/P2 ($1.697 \pm 0.103$), P1/P15 ($1.664 \pm 0.120$), P9/P21 ($1.685 \pm 0.320$), P10/P22 ($1.691 \pm 0.418$), P12/P22 ($1.691 \pm 0.418$), P18/P13 ($1.661 \pm 0.284$), and P18/P20 ($1.695 \pm 0.401$); however, these ratios differed significantly from the golden ratio. The findings provide valuable insights into the relationship between atlas morphometric ratios and the golden ratio in this Turkish population sample. Several ratios were found to be numerically close to the golden ratio. These results provide reference data on atlas morphometry and suggest that selected proportional relationships of the atlas may reflect its distinctive anatomical organization.

**KEY WORDS: Atlas morphometry, Fibonacci series, Golden ratio, Symmetry, Turkish population**

## INTRODUCTION

The cervical region of the vertebral column comprises seven vertebra, sequentially numbered from C1 to C7. While they generally share similar morphological characteristics, certain vertebra in the cervical region exhibit distinctive structural differences, classifying them as atypical vertebra (Kolenkiewicz *et al*., 2018). The first cervical vertebra, the atlas, is one of these atypical vertebra and is characterized by the absence of a vertebral body and spinous process (Sertel Meyvaci *et al*., 2020). A literature review indicates that, in addition to its anatomical significance, the atlas also exhibits sexually dimorphic characteristics (Sanabria Medina *et al*., 2011: Padovan *et al*., 2019). The golden ratio (phi or F) represents a value that is aesthetically pleasing to the human eye (Walker *et al*., 2011). With an approximate value of 1.618, the golden ratio was first described in antiquity by Pythagoras and later developed by Leonardo Pisano Fibonacci in 1202 (Henein *et al*., 2011; Benavoli *et al*., 2009). The golden ratio is obtained by dividing a line into two segments: when the longer segment (a) is divided by the shorter segment (b), and the sum of both segments (a + b) is divided by the longer segment (a), the result is 1:1.618 (Walker *et al*., 2011). Both the golden ratio and the associated golden angle of 137.5° have been identified in certain proportions and angles within the human body and nature (Henein *et al*., 2011). Studies have demonstrated that the golden ratio appears not only in the human genome (Yamagishi *et al*., 2008) and cellular structure (Purnell *et al*., 2018) but also in various physical characteristics, such as gait mechanics (Iosa *et al*., 2013; Iosa *et al*., 2016) and the aesthetic dimensions of the face (Bashour, 2006; Kim, 2007; Lipiec *et al*., 2019). Furthermore, it has been utilized in aesthetic surgical procedures on different body regions to determine the ideal proportions (Raposio *et al*., 2024).

[1] Department of Anatomy, Faculty of Medicine, Bolu Abant Izzet Baysal University, Bolu, Turkiye.
[2] Department of Biostatistics and Medical Informatics, Faculty of Medicine, Istanbul Medeniyet University, Istanbul, Turkiye.
[3] Department of Oral and Maxillofacial Radiology, Faculty of Dentistry, Bolu Abant Izzet Baysal University, Bolu, Turkiye.
[4] Basaksehir Oral and Dental Health Care Center, Istanbul, Turkiye.

Received: 2025-02-28 Accepted: 2026-02-24

Although the golden ratio has been evaluated in different anatomical regions, its possible relationship with the morphometric parameters of the atlas has not been sufficiently investigated. Therefore, the present study aimed to evaluate whether selected morphometric ratios of the atlas conform to the golden ratio by analyzing anatomical landmarks and parameters specific to its unique morphology.

## MATERIAL AND METHOD

This study retrospectively analyzed cone-beam computed tomography (CBCT) images of 359 individuals, including 180 males and 179 females, aged 18–82 years, who presented to the Department of Oral and Maxillofacial Radiology, Faculty of Dentistry, Bolu Abant Izzet Baysal University, between 2020 and 2024. The images were evaluated to assess the morphometric parameters of the atlas. Ethical approval for the study was obtained from the Bolu Abant Izzet Baysal University Non-Interventional Clinical Research Ethics Committee with decision number 2024/382. The ratios between the parameters were calculated to investigate their conformity to the golden ratio. In this study, cases were classified into 4 groups based on the mean (XX) of each evaluated ratio, considering the corresponding standard deviation (SD) (Sertel Meyvaci *et al*., 2021).

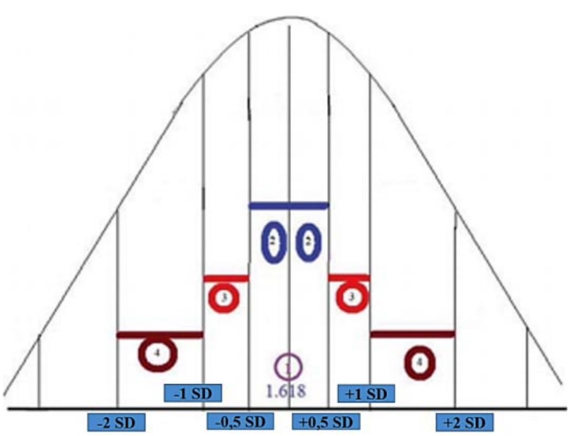


Fig. 1. Groups formed based on deviations from the mean of the evaluated ratios.

- The first group included cases that were exactly aligned with the golden ratio (1.618).
- The second group comprised cases within a range of ± 0.5 standard deviations from the mean ratio (XX-0.5 SD to XX+0.5 SD).
- The third group included cases with deviations from the golden ratio between ± 0.5 SD and ± 1 SD (at least 0.5 SD and at most 1 SD away).
- The fourth group consisted of cases with deviations between ± 1 SD and ± 2 SD from the golden ratio (at least 1 SD and at most 2 SD away).

The classification of these groups is graphically summarized in Figure 1.

A total of 22 parameters previously defined as atlas-specific (Sertel Meyvaci *et al*., 2024); were measured on facial CBCT images, and 57 ratios were calculated based on these measurements.

### Measurement of Parameters

The parameters were measured in millimeters (mm) on multiplanar and three-dimensional CBCT images using predefined reference points, with measurements recorded to one decimal place. The description of the 22 parameters used in this study are provided below (Table I).

Table I. Description of anatomic parameters of the atlas.

| Parameters | Definition |
|---|---|
| **P1** | Maximum transverse diameter |
| **P2** | Maximum anteroposterior diameter |
| **P3** | Transverse diameter of vertebral foramen |
| **P4** | Anteroposterior diameter of vertebral foramen |
| **P5** | The inner diameter of the transverse foramen |
| **P6** | The outer diameter of the transverse foramen |
| **P7** | Maximum anteroposterior diameter of the right superior articular surface |
| **P8** | Maximum anteroposterior diameter of the left superior articular surface |
| **P9** | Minimum mediolateral diameter of the right superior articular surface |
| **P10** | Minimum mediolateral diameter of left superior articular surface |
| **P11** | Maximum anteroposterior diameter of the right inferior articular surface |
| **P12** | Maximum anteroposterior diameter of left inferior articular surface |
| **P13** | Minimum mediolateral diameter of the right inferior articular surface |
| **P14** | Minimum mediolateral diameter of left inferior articular surface |
| **P15** | Maximum distance between the lateral edges of the superior articular surfaces |
| **P16** | Minimum distance between the lateral edges of the superior articular surfaces |
| **P17** | Maximum distance between the lateral edges of the inferior articular surfaces |
| **P18** | Minimum distance between the lateral edges of the inferior articular surfaces |
| **P19** | Height of the anterior arcus |
| **P20** | Height of the posterior arcus |
| **P21** | Diameter of the anterior arcus |
| **P22** | The diameter of the posterior arcus |

The ratios calculated using the 22 measured parameters are as follows:

**1)** P1/P2, **2)** P1/P5, **3)** P1/P15, **4)** P1/P17, **5)** P4/P16, **6)** P4/P18, **7)** P5/P3, **8)** P5/P4 **9)** P6/17 **10)** P7/P9 **11)** P7/P11 **12)** P7/P13 **13)** P7/P19 **14)** P7/P20 **15)** P7/P22 **16)** P8/P10 **17)** P8/P12 **18)** P8/P14 **19)** P8/P19 **20)** P8/P20 **21)** P8/P22 **22)** P9/P21 **23)** P9/P22 **24)** P10/P21 **25)** P10/P22 **26)** P11/P21 **27)** P11/P22 **28)** P12/P21 **29)** P12/P22 **30)** P13/P21 **31)** P13/P22 **32)** P14/P21 **33)** P14/P22 **34)** P15/P3 **35)** P15/P4 **36)** P16/P9 **37)** P16/P10 **38)** P16/P11 **39)** P16/P12 **40)** P16/P13 **41)** P16/P14 **42)** P16/P19 **43)** P16/P20 **44)** P17/P3 **45)** P17/P4 **46)** P18/P9 **47)** P18/P10 **48)** P18/P11 **49)** P18/P12 **50)** P18/P13 **51)** P18/P14 **52)** P18/P19 **53)** P18/P20 **54)** P19/P21 **55)** P19/P22 **56)** P20/P21 **57)** P20/P22

These calculated ratios were used to evaluate the proportional relationships among atlas parameters and to determine their conformity to the golden ratio. Each ratio was compared with the golden ratio value of 1.618, and deviations from this value were subsequently analyzed statistically.

### Statistical Analysis

Descriptive statistics were calculated for the measurements and derived ratios, including mean, standard deviation (SD), median, 25th and 75th percentiles, counts, and percentage frequencies where appropriate. The normality of the data was assessed using the Kolmogorov–Smirnov test. The deviation of each calculated ratio from the golden ratio value of 1.618 was analyzed using the One-Sample t-test. In addition, individuals were classified into groups according to their deviation from the golden ratio at 0.5 SD, 1.0 SD, and 2.0 SD levels. The sex distribution of these deviation groups was then examined. The Pearson chi-square test was used to compare males and females in terms of their distribution across the deviation groups. A p-value of $\leq 0.05$ was considered statistically significant. All statistical analyses were performed using SPSS version 29.

## RESULTS

The individuals included in the study were aged between 18 and 82 years, with a mean age of 40.1 ± 16.7 years. The study population consisted of 180 males and 179 females. A total of 57 ratios were calculated based on the obtained measurements. Descriptive statistics for these ratios in the overall study population are presented in Table II. Using the SD values provided in this table, deviation ranges from the golden ratio value of 1.618 were determined at ± 0.5 SD, ± 1.0 SD, and ± 2.0 SD levels. Values outside the ± 2.0 SD range were classified as a separate group.

When examining whether the 57 ratios significantly deviated from the reported golden ratio (1.618), it was found that only the P9/P22 and P18/P14 ratios did not show a statistically significant deviation, whereas all other ratios exhibited a significant deviation (Table III).

In Table III, the mean difference column presents the average deviation of each calculated ratio from the golden ratio. Positive mean difference values indicate that the calculated ratio is significantly greater than the golden ratio, whereas negative values indicate that the calculated ratio is significantly smaller than the golden ratio.

An analysis of the distribution of the 57 ratios at various SD levels around the golden ratio (1.618) was conducted. For each of the 57 calculated ratios, deviations from the golden ratio at 0.5 SD, 1.0 SD, and 2.0 SD were determined, and groups were formed accordingly. The distribution of these groups across all individuals is presented in Table IV. The groups consist of cases deviating by 0.5 SD, 1.0 SD, 2.0 SD, and those deviating more than 2.0 SD from the golden ratio. Notably, none of the ratios were found to be exactly equal to 1.618.

An analysis of the distribution frequencies of the 57 ratios at various SD levels around the golden ratio (1.618) in relation to sex differences was conducted. When the distribution of these ratio groups was examined, those with results that differed according to sex ($p > 0.05$) are presented in Table V.

Table V displays the distribution of SD deviation groups for each calculated ratio according to sex. Groups that exhibited statistically significant differences between sexes are indicated with completely different letters (a and b).

## DISCUSSION

The golden ratio (phi or F) is a mathematical proportion that has been recognized for centuries, with numerous studies demonstrating that many structures in nature follow this principle (Mahakul & Agarwal, 2021). In the human body, this divine ratio has been associated with enhancing aesthetic perception and optimizing functional capacity (Iosa *et al*., 2016). A study investigating the relationship between anthropometry and gait dynamics confirmed the hypothesis that physiological human gait follows the golden ratio in the proportionality of stance and swing phases. This finding supports the notion that the golden ratio naturally exists within the human body (Iosa *et al*., 2016). Similarly, it has been demonstrated that the ratio of forearm length to hand length is also 1.618 (Stakhov & Sluchenkova, 2002).

Table II. Descriptive statistics of the calculated ratios.

| | n | Mean | SD | Minimum | Maximum | Percentiles | | |
|---|---|---|---|---|---|---|---|---|
| | | | | | | 25 | Median | 75 |
| P1/P2 | 359 | 1.697 | 0.103 | 1.426 | 2.000 | 1.627 | 1.691 | 1.761 |
| P1/P5 | 359 | 1.713 | 0.092 | 1.333 | 2.253 | 1.659 | 1.711 | 1.769 |
| P1/P15 | 359 | 1.664 | 0.120 | 1.373 | 2.053 | 1.575 | 1.660 | 1.740 |
| P1/P17 | 359 | 1.785 | 0.103 | 1.505 | 2.154 | 1.714 | 1.787 | 1.847 |
| P4/P16 | 359 | 1.875 | 0.237 | 1.244 | 2.571 | 1.733 | 1.875 | 2.022 |
| P4/P18 | 359 | 1.965 | 0.238 | 1.242 | 2.837 | 1.796 | 1.969 | 2.125 |
| P5/P3 | 359 | 1.483 | 0.126 | 1.021 | 2.000 | 1.402 | 1.474 | 1.556 |
| P5/P4 | 359 | 1.443 | 0.125 | 0.943 | 2.195 | 1.369 | 1.441 | 1.516 |
| P6/P17 | 359 | 1.385 | 0.101 | 0.811 | 1.715 | 1.329 | 1.388 | 1.445 |
| P7/P9 | 359 | 1.332 | 0.161 | 0.972 | 2.059 | 1.220 | 1.316 | 1.429 |
| P7/P11 | 359 | 1.246 | 0.127 | 1.000 | 1.683 | 1.150 | 1.233 | 1.318 |
| P7/P13 | 359 | 1.478 | 0.166 | 0.971 | 1.960 | 1.364 | 1.467 | 1.579 |
| P7/P19 | 359 | 1.248 | 0.192 | 0.806 | 1.923 | 1.111 | 1.227 | 1.355 |
| P7/P20 | 359 | 1.509 | 0.270 | 0.900 | 2.957 | 1.310 | 1.470 | 1.667 |
| P7/P22 | 359 | 1.509 | 0.270 | 0.900 | 2.957 | 1.310 | 1.470 | 1.667 |
| P8/P10 | 359 | 1.300 | 0.159 | 0.843 | 1.827 | 1.200 | 1.286 | 1.411 |
| P8/P12 | 359 | 1.264 | 0.122 | 1.000 | 1.810 | 1.176 | 1.250 | 1.341 |
| P8/P14 | 359 | 1.440 | 0.156 | 0.939 | 1.917 | 1.323 | 1.435 | 1.545 |
| P8/P19 | 359 | 1.233 | 0.192 | 0.794 | 1.833 | 1.111 | 1.196 | 1.333 |
| P8/P20 | 359 | 1.490 | 0.270 | 0.813 | 2.880 | 1.313 | 1.467 | 1.667 |
| P8/P22 | 359 | 2.124 | 0.500 | 1.042 | 3.825 | 1.750 | 2.077 | 2.460 |
| P9/P21 | 359 | 1.685 | 0.320 | 0.970 | 2.867 | 1.462 | 1.667 | 1.900 |
| P9/P22 | 359 | 1.637 | 0.434 | 0.808 | 3.273 | 1.304 | 1.565 | 1.943 |
| P10/P21 | 359 | 1.747 | 0.326 | 0.909 | 2.720 | 1.538 | 1.714 | 1.947 |
| P10/P22 | 359 | 1.691 | 0.418 | 0.818 | 3.545 | 1.400 | 1.643 | 1.962 |
| P11/P21 | 359 | 1.795 | 0.331 | 1.061 | 2.773 | 1.542 | 1.769 | 2.000 |
| P11/P22 | 359 | 1.735 | 0.411 | 0.818 | 3.455 | 1.438 | 1.688 | 2.000 |
| P12/P21 | 359 | 1.747 | 0.326 | 0.909 | 2.720 | 1.538 | 1.714 | 1.947 |
| P12/P22 | 359 | 1.691 | 0.418 | 0.818 | 3.545 | 1.400 | 1.643 | 1.962 |
| P13/P21 | 359 | 1.520 | 0.302 | 0.828 | 2.688 | 1.300 | 1.500 | 1.700 |
| P13/P22 | 359 | 1.470 | 0.369 | 0.738 | 2.545 | 1.188 | 1.417 | 1.700 |
| P14/P21 | 359 | 1.537 | 0.292 | 0.839 | 2.333 | 1.320 | 1.500 | 1.714 |
| P14/P22 | 359 | 1.488 | 0.373 | 0.738 | 2.550 | 1.217 | 1.429 | 1.731 |
| P15/P3 | 359 | 1.529 | 0.133 | 1.093 | 1.945 | 1.448 | 1.518 | 1.620 |
| P15/P4 | 359 | 1.489 | 0.138 | 1.102 | 2.293 | 1.394 | 1.485 | 1.583 |
| P16/P9 | 359 | 1.566 | 0.245 | 1.000 | 2.500 | 1.400 | 1.528 | 1.700 |
| P16/P10 | 359 | 1.547 | 0.235 | 1.074 | 2.439 | 1.375 | 1.525 | 1.683 |
| P16/P11 | 359 | 1.468 | 0.233 | 1.000 | 2.857 | 1.303 | 1.447 | 1.591 |
| P16/P12 | 359 | 1.508 | 0.222 | 1.023 | 2.609 | 1.360 | 1.487 | 1.625 |
| P16/P13 | 359 | 1.739 | 0.278 | 1.209 | 3.333 | 1.549 | 1.710 | 1.882 |
| P16/P14 | 359 | 1.715 | 0.257 | 1.200 | 3.226 | 1.528 | 1.686 | 1.857 |
| P16/P19 | 359 | 1.469 | 0.275 | 0.897 | 2.645 | 1.267 | 1.425 | 1.616 |
| P16/P20 | 359 | 1.781 | 0.436 | 0.900 | 6.000 | 1.500 | 1.700 | 1.988 |
| P17/P3 | 359 | 1.423 | 0.119 | 1.092 | 1.800 | 1.340 | 1.431 | 1.500 |
| P17/P4 | 359 | 1.385 | 0.122 | 1.098 | 2.195 | 1.303 | 1.378 | 1.464 |
| P18/P9 | 359 | 1.494 | 0.242 | 0.862 | 2.444 | 1.341 | 1.474 | 1.625 |
| P18/P10 | 359 | 1.476 | 0.231 | 0.926 | 2.370 | 1.324 | 1.471 | 1.615 |
| P18/P11 | 359 | 1.399 | 0.219 | 0.933 | 2.762 | 1.250 | 1.391 | 1.524 |
| P18/P12 | 359 | 1.437 | 0.211 | 0.903 | 2.522 | 1.310 | 1.429 | 1.550 |
| P18/P13 | 359 | 1.661 | 0.284 | 1.075 | 3.222 | 1.465 | 1.636 | 1.814 |
| P18/P14 | 359 | 1.638 | 0.263 | 1.097 | 3.118 | 1.455 | 1.606 | 1.778 |
| P18/P19 | 359 | 1.398 | 0.251 | 0.755 | 2.444 | 1.225 | 1.375 | 1.538 |
| P18/P20 | 359 | 1.695 | 0.401 | 0.957 | 5.800 | 1.455 | 1.636 | 1.875 |
| P19/P21 | 359 | 1.794 | 0.275 | 1.157 | 3.000 | 1.600 | 1.754 | 1.955 |
| P19/P22 | 359 | 1.748 | 0.443 | 0.877 | 3.500 | 1.402 | 1.692 | 2.040 |
| P20/P21 | 359 | 1.501 | 0.291 | 0.714 | 2.400 | 1.308 | 1.467 | 1.667 |
| P20/P22 | 359 | 1.445 | 0.334 | 0.762 | 3.000 | 1.207 | 1.400 | 1.662 |

Table III. Comparison of the calculated ratios against the golden ratio.

| | Test Value = 1.618 | | | | | |
|---|---|---|---|---|---|---|
| | t | df | P | Mean Difference | 95% Confidence Interval of the Difference | |
| | | | | | Lower | Upper |
| P1/P2 | 14.413 | 358 | <0.001 | 0.079 | 0.068 | 0.089 |
| P1/P5 | 19.704 | 358 | <0.001 | 0.095 | 0.086 | 0.105 |
| P1/P15 | 7.183 | 358 | <0.001 | 0.046 | 0.033 | 0.058 |
| P1/P17 | 30.818 | 358 | <0.001 | 0.167 | 0.156 | 0.178 |
| P4/P16 | 20.504 | 358 | <0.001 | 0.257 | 0.232 | 0.281 |
| P4/P18 | 27.658 | 358 | <0.001 | 0.347 | 0.323 | 0.372 |
| P5/P3 | -20.362 | 358 | <0.001 | -0.135 | -0.148 | -0.122 |
| P5/P4 | -26.615 | 358 | <0.001 | -0.175 | -0.188 | -0.162 |
| P6/P17 | -43.752 | 358 | <0.001 | -0.233 | -0.243 | -0.222 |
| P7/P9 | -33.717 | 358 | <0.001 | -0.286 | -0.303 | -0.270 |
| P7/P11 | -55.419 | 358 | <0.001 | -0.372 | -0.385 | -0.359 |
| P7/P13 | -16.062 | 358 | <0.001 | -0.140 | -0.158 | -0.123 |
| P7/P19 | -36.374 | 358 | <0.001 | -0.370 | -0.389 | -0.350 |
| P7/P20 | -7.665 | 358 | <0.001 | -0.109 | -0.137 | -0.081 |
| P7/P22 | -7.665 | 358 | <0.001 | -0.109 | -0.137 | -0.081 |
| P8/P10 | -37.942 | 358 | <0.001 | -0.318 | -0.334 | -0.301 |
| P8/P12 | -54.997 | 358 | <0.001 | -0.354 | -0.366 | -0.341 |
| P8/P14 | -21.595 | 358 | <0.001 | -0.178 | -0.194 | -0.161 |
| P8/P19 | -38.038 | 358 | <0.001 | -0.385 | -0.405 | -0.365 |
| P8/P20 | -8.948 | 358 | <0.001 | -0.128 | -0.156 | -0.100 |
| P8/P22 | 19.148 | 358 | <0.001 | 0.506 | 0.454 | 0.558 |
| P9/P21 | 3.989 | 358 | <0.001 | 0.067 | 0.034 | 0.101 |
| P9/P22 | 0.824 | 358 | 0.410 | 0.019 | -0.026 | 0.064 |
| P10/P21 | 7.507 | 358 | <0.001 | 0.129 | 0.095 | 0.163 |
| P10/P22 | 3.295 | 358 | 0.001 | 0.073 | 0.029 | 0.116 |
| P11/P21 | 10.159 | 358 | <0.001 | 0.177 | 0.143 | 0.212 |
| P11/P22 | 5.391 | 358 | <0.001 | 0.117 | 0.074 | 0.160 |
| P12/P21 | 7.507 | 358 | <0.001 | 0.129 | 0.095 | 0.163 |
| P12/P22 | 3.295 | 358 | 0.001 | 0.073 | 0.029 | 0.116 |
| P13/P21 | -6.142 | 358 | <0.001 | -0.098 | -0.129 | -0.067 |
| P13/P22 | -7.604 | 358 | <0.001 | -0.148 | -0.186 | -0.110 |
| P14/P21 | -5.254 | 358 | <0.001 | -0.081 | -0.111 | -0.051 |
| P14/P22 | -6.595 | 358 | <0.001 | -0.130 | -0.168 | -0.091 |
| P15/P3 | -12.663 | 358 | <0.001 | -0.089 | -0.103 | -0.075 |
| P15/P4 | -17.772 | 358 | <0.001 | -0.129 | -0.144 | -0.115 |
| P16/P9 | -4.032 | 358 | <0.001 | -0.052 | -0.078 | -0.027 |
| P16/P10 | -5.718 | 358 | <0.001 | -0.071 | -0.095 | -0.046 |
| P16/P11 | -12.153 | 358 | <0.001 | -0.150 | -0.174 | -0.125 |
| P16/P12 | -9.398 | 358 | <0.001 | -0.110 | -0.133 | -0.087 |
| P16/P13 | 8.246 | 358 | <0.001 | 0.121 | 0.092 | 0.150 |
| P16/P14 | 7.167 | 358 | <0.001 | 0.097 | 0.071 | 0.124 |
| P16/P19 | -10.273 | 358 | <0.001 | -0.149 | -0.178 | -0.121 |
| P16/P20 | 7.081 | 358 | <0.001 | 0.163 | 0.118 | 0.208 |
| P17/P3 | -31.047 | 358 | <0.001 | -0.195 | -0.207 | -0.183 |
| P17/P4 | -36.169 | 358 | <0.001 | -0.233 | -0.245 | -0.220 |
| P18/P9 | -9.743 | 358 | <0.001 | -0.124 | -0.149 | -0.099 |
| P18/P10 | -11.663 | 358 | <0.001 | -0.142 | -0.166 | -0.118 |
| P18/P11 | -18.972 | 358 | <0.001 | -0.219 | -0.242 | -0.196 |
| P18/P12 | -16.229 | 358 | <0.001 | -0.181 | -0.203 | -0.159 |
| P18/P13 | 2.842 | 358 | 0.005 | 0.043 | 0.013 | 0.072 |
| P18/P14 | 1.413 | 358 | 0.159 | 0.020 | -0.008 | 0.047 |
| P18/P19 | -16.567 | 358 | <0.001 | -0.220 | -0.246 | -0.194 |
| P18/P20 | 3.628 | 358 | <0.001 | 0.077 | 0.035 | 0.118 |
| P19/P21 | 12.100 | 358 | <0.001 | 0.176 | 0.147 | 0.204 |
| P19/P22 | 5.579 | 358 | <0.001 | 0.130 | 0.084 | 0.176 |
| P20/P21 | -7.631 | 358 | <0.001 | -0.117 | -0.147 | -0.087 |
| P20/P22 | -9.827 | 358 | <0.001 | -0.173 | -0.208 | -0.139 |

Table IV. Distribution of ratios based on their deviation from the golden ratio.

| SD range | | % | n | | % | n | | % | n |
|---|---|---|---|---|---|---|---|---|---|
| ± 0.5 SD range | **P1/P2** | 114 | 31.8 | **P8/P20** | 121 | 33.7 | **P16/P12** | 116 | 32.3 |
| 0.5 - 1.0 SD range | | 90 | 25.1 | | 104 | 29.0 | | 108 | 30.1 |
| 1.0 - 2.0 SD range | | 114 | 31.8 | | 117 | 32.6 | | 112 | 31.2 |
| + 2.0 SD range | | 41 | 11.4 | | 17 | 4.7 | | 23 | 6.4 |
| ± 0.5 SD range | **P1/P5** | 77 | 21.4 | **P8/P22** | 106 | 29.5 | **P16/P13** | 145 | 40.4 |
| 0.5 - 1.0 SD range | | 90 | 25.1 | | 83 | 23.1 | | 121 | 33.7 |
| 1.0 - 2.0 SD range | | 134 | 37.3 | | 111 | 30.9 | | 74 | 20.6 |
| + 2.0 SD range | | 58 | 16.2 | | 59 | 16.4 | | 19 | 5.3 |
| ± 0.5 SD range | **P1/P15** | 136 | 37.9 | **P9/P21** | 146 | 40.7 | **P16/P14** | 155 | 43.2 |
| 0.5 - 1.0 SD range | | 99 | 27.6 | | 100 | 27.9 | | 107 | 29.8 |
| 1.0 - 2.0 SD range | | 102 | 28.4 | | 94 | 26.2 | | 77 | 21.4 |
| + 2.0 SD range | | 22 | 6.1 | | 19 | 5.3 | | 20 | 5.6 |
| ± 0.5 SD range | **P1/P17** | 43 | 12.0 | **P9/P22** | 121 | 33.7 | **P16/P19** | 95 | 26.5 |
| 0.5 - 1.0 SD range | | 52 | 14.5 | | 128 | 35.7 | | 107 | 29.8 |
| 1.0 - 2.0 SD range | | 150 | 41.8 | | 96 | 26.7 | | 140 | 39.0 |
| + 2.0 SD range | | 114 | 31.8 | | 14 | 3.9 | | 17 | 4.7 |
| ± 0.5 SD range | **P4/P16** | 67 | 18.7 | **P10/P21** | 144 | 40.1 | **P16/P20** | 185 | 51.5 |
| 0.5 - 1.0 SD range | | 84 | 23.4 | | 97 | 27.0 | | 98 | 27.3 |
| 1.0 - 2.0 SD range | | 152 | 42.3 | | 92 | 25.6 | | 60 | 16.7 |
| + 2.0 SD range | | 56 | 15.6 | | 26 | 7.2 | | 16 | 4.5 |
| ± 0.5 SD range | **P4/P18** | 60 | 16.7 | **P10/P22** | 153 | 42.6 | **P17/P3** | 32 | 8.9 |
| 0.5 - 1.0 SD range | | 55 | 15.3 | | 91 | 25.3 | | 63 | 17.5 |
| 1.0 - 2.0 SD range | | 141 | 39.3 | | 100 | 27.9 | | 137 | 38.2 |
| + 2.0 SD range | | 103 | 28.7 | | 15 | 4.2 | | 127 | 35.4 |
| ± 0.5 SD range | **P5/P3** | 72 | 20.1 | **P11/P21** | 136 | 37.9 | **P17/P4** | 26 | 7.2 |
| 0.5 - 1.0 SD range | | 74 | 20.6 | | 101 | 28.1 | | 28 | 7.8 |
| 1.0 - 2.0 SD range | | 150 | 41.8 | | 86 | 24.0 | | 136 | 37.9 |
| + 2.0 SD range | | 63 | 17.5 | | 36 | 10.1 | | 169 | 47.1 |
| ± 0.5 SD range | **P5/P4** | 47 | 13.1 | **P11/P22** | 145 | 40.4 | **P18/P9** | 112 | 31.2 |
| 0.5 - 1.0 SD range | | 64 | 17.8 | | 103 | 28.7 | | 113 | 31.5 |
| 1.0 - 2.0 SD range | | 159 | 44.3 | | 85 | 23.7 | | 113 | 31.5 |
| + 2.0 SD range | | 89 | 24.8 | | 26 | 7.2 | | 21 | 5.8 |
| ± 0.5 SD range | **P6/P17** | 11 | 3.1 | **P12/P21** | 144 | 40.1 | **P18/P10** | 105 | 29.2 |
| 0.5 - 1.0 SD range | | 17 | 4.7 | | 97 | 27.0 | | 107 | 29.8 |
| 1.0 - 2.0 SD range | | 105 | 29.2 | | 92 | 25.6 | | 116 | 32.3 |
| + 2.0 SD range | | 226 | 63.0 | | 26 | 7.2 | | 31 | 8.6 |
| ± 0.5 SD range | **P7/P9** | 27 | 7.5 | **P12/P22** | 153 | 42.6 | **P18/P11** | 69 | 19.2 |
| 0.5 - 1.0 SD range | | 48 | 13.4 | | 91 | 25.3 | | 93 | 25.9 |
| 1.0 - 2.0 SD range | | 121 | 33.7 | | 100 | 27.9 | | 143 | 39.8 |
| + 2.0 SD range | | 163 | 45.4 | | 15 | 4.2 | | 54 | 15.0 |
| ± 0.5 SD range | **P7/P11** | 8 | 2.2 | **P13/P21** | 120 | 33.4 | **P18/P12** | 93 | 25.9 |
| 0.5 - 1.0 SD range | | 9 | 2.5 | | 108 | 30.1 | | 90 | 25.1 |
| 1.0 - 2.0 SD range | | 45 | 12.5 | | 115 | 32.0 | | 132 | 36.8 |
| + 2.0 SD range | | 297 | 82.7 | | 16 | 4.5 | | 44 | 12.3 |
| ± 0.5 SD range | **P7/P13** | 82 | 22.8 | **P13/P22** | 104 | 29.0 | **P18/P13** | 145 | 40.4 |
| 0.5 - 1.0 SD range | | 98 | 27.3 | | 104 | 29.0 | | 119 | 33.1 |
| 1.0 - 2.0 SD range | | 134 | 37.3 | | 138 | 38.4 | | 79 | 22.0 |
| + 2.0 SD range | | 45 | 12.5 | | 13 | 3.6 | | 16 | 4.5 |
| ± 0.5 SD range | **P7/P19** | 31 | 8.6 | **P14/P21** | 120 | 33.4 | **P18/P14** | 148 | 41.2 |
| 0.5 - 1.0 SD range | | 29 | 8.1 | | 107 | 29.8 | | 113 | 31.5 |
| 1.0 - 2.0 SD range | | 111 | 30.9 | | 116 | 32.3 | | 86 | 24.0 |
| + 2.0 SD range | | 188 | 52.4 | | 16 | 4.5 | | 12 | 3.3 |
| ± 0.5 SD range | **P7/P20** | 117 | 32.6 | **P14/P22** | 104 | 29.0 | **P18/P19** | 77 | 21.4 |
| 0.5 - 1.0 SD range | | 100 | 27.9 | | 106 | 29.5 | | 82 | 22.8 |
| 1.0 - 2.0 SD range | | 129 | 35.9 | | 137 | 38.2 | | 160 | 44.6 |
| + 2.0 SD range | | 13 | 3.6 | | 12 | 3.3 | | 40 | 11.1 |
| ± 0.5 SD range | **P7/P22** | 117 | 32.6 | **P15/P3** | 105 | 29.2 | **P18/P20** | 172 | 47.9 |
| 0.5 - 1.0 SD range | | 100 | 27.9 | | 96 | 26.7 | | 122 | 34.0 |
| 1.0 - 2.0 SD range | | 129 | 35.9 | | 117 | 32.6 | | 53 | 14.8 |
| + 2.0 SD range | | 13 | 3.6 | | 41 | 11.4 | | 12 | 3.3 |
| ± 0.5 SD range | **P8/P10** | 13 | 3.6 | **P15/P4** | 93 | 25.9 | **P19/P21** | 142 | 39.6 |
| 0.5 - 1.0 SD range | | 40 | 11.1 | | 84 | 23.4 | | 92 | 25.6 |
| 1.0 - 2.0 SD range | | 111 | 30.9 | | 134 | 37.3 | | 93 | 25.9 |
| + 2.0 SD range | | 195 | 54.3 | | 48 | 13.4 | | 32 | 8.9 |
| ± 0.5 SD range | **P8/P12** | 5 | 1.4 | **P16/P9** | 135 | 37.6 | **P19/P22** | 135 | 37.6 |
| 0.5 - 1.0 SD range | | 10 | 2.8 | | 119 | 33.1 | | 115 | 32.0 |
| 1.0 - 2.0 SD range | | 52 | 14.5 | | 87 | 24.2 | | 91 | 25.3 |
| + 2.0 SD range | | 292 | 81.3 | | 18 | 5.0 | | 18 | 5.0 |
| ± 0.5 SD range | **P8/P14** | 71 | 19.8 | **P16/P10** | 123 | 34.3 | **P20/P21** | 114 | 31.8 |
| 0.5 - 1.0 SD range | | 72 | 20.1 | | 111 | 30.9 | | 115 | 32.0 |
| 1.0 - 2.0 SD range | | 139 | 38.7 | | 108 | 30.1 | | 108 | 30.1 |
| + 2.0 SD range | | 77 | 21.4 | | 17 | 4.7 | | 22 | 6.1 |
| ± 0.5 SD range | **P8/P19** | 26 | 7.2 | **P16/P11** | 99 | 27.6 | **P20/P22** | 102 | 28.4 |
| 0.5 - 1.0 SD range | | 28 | 7.8 | | 108 | 30.1 | | 110 | 30.6 |
| 1.0 - 2.0 SD range | | 102 | 28.4 | | 126 | 35.1 | | 126 | 35.1 |
| + 2.0 SD range | | 203 | 56.5 | | 26 | 7.2 | | 21 | 5.8 |

Table V. Distribution of groups showing various SD deviations from the golden ratio by sex.

| SD range | | Male | | Female | | |
|---|---|---|---|---|---|---|
| | | n | % | n | % | P |
| **P1/P5** | ± 0.5 SD range | 34 | 18.9 | 43 | 24.0 | **0.039** |
| | 0.5 - 1.0 SD range | 37 | 20.6[a] | 53 | 29.6[b] | |
| | 1.0 - 2.0 SD range | 73 | 40.6 | 61 | 34.1 | |
| | + 2.0 SD range | 36 | 20.0[a] | 22 | 12.3[b] | |
| **P1/P17** | ± 0.5 SD range | 16 | 8.9 | 27 | 15.1 | **0.001** |
| | 0.5 - 1.0 SD range | 15 | 8.3[a] | 37 | 20.7[b] | |
| | 1.0 - 2.0 SD range | 84 | 46.7 | 66 | 36.9 | |
| | + 2.0 SD range | 65 | 36.1 | 49 | 27.4 | |
| **P4/P18** | ± 0.5 SD range | 16 | 8.9[a] | 44 | 24.6[b] | **0.001** |
| | 0.5 - 1.0 SD range | 32 | 17.8 | 23 | 12.8 | |
| | 1.0 - 2.0 SD range | 70 | 38.9 | 71 | 39.7 | |
| | + 2.0 SD range | 62 | 34.4[a] | 41 | 22.9[b] | |
| **P7/P19** | ± 0.5 SD range | 12 | 6.7 | 19 | 10.6 | **0.014** |
| | 0.5 - 1.0 SD range | 8 | 4.4[a] | 21 | 11.7[b] | |
| | 1.0 - 2.0 SD range | 54 | 30.0 | 57 | 31.8 | |
| | + 2.0 SD range | 106 | 58.9[a] | 82 | 45.8[b] | |
| **P8/P14** | ± 0.5 SD range | 46 | 25.6[a] | 25 | 14.0[b] | **0.023** |
| | 0.5 - 1.0 SD range | 31 | 17.2 | 41 | 22.9 | |
| | 1.0 - 2.0 SD range | 62 | 34.4 | 77 | 43.0 | |
| | + 2.0 SD range | 41 | 22.8 | 36 | 20.1 | |
| **P8/P19** | ± 0.5 SD range | 7 | 3.9[a] | 19 | 10.6[b] | **0.008** |
| | 0.5 - 1.0 SD range | 11 | 6.1 | 17 | 9.5 | |
| | 1.0 - 2.0 SD range | 46 | 25.6 | 56 | 31.3 | |
| | + 2.0 SD range | 116 | 64.4[a] | 87 | 48.6[b] | |
| **P16/P20** | ± 0.5 SD range | 93 | 51.7 | 92 | 51.4 | **0.050** |
| | 0.5 - 1.0 SD range | 55 | 30.6 | 43 | 24.0 | |
| | 1.0 - 2.0 SD range | 29 | 16.1 | 31 | 17.3 | |
| | + 2.0 SD range | 3 | 1.7[a] | 13 | 7.3[b] | |
| **P18/P19** | ± 0.5 SD range | 28 | 15.6[a] | 49 | 27.4[b] | **0.050** |
| | 0.5 - 1.0 SD range | 43 | 23.9 | 39 | 21.8 | |
| | 1.0 - 2.0 SD range | 86 | 47.8 | 74 | 41.3 | |
| | + 2.0 SD range | 23 | 12.8 | 17 | 9.5 | |

In a study testing, whether the lengths of metacarpal and phalangeal bones align with the Fibonacci sequence, conformity to the golden ratio was observed only between the metacarpal and proximal phalanx of the little finger. However, the absence of a similar relationship in other bones was attributed to differences in measurement techniques, specifically whether the measurements were taken along the joint line or through the center of joint rotation (Park *et al*., 2003). The golden ratio has also been proposed to play a crucial role not only in the structural organization of human anatomy but also in the functioning of various body systems. For instance, the ratio of uterine length to width in a non-pregnant uterus has been reported to decrease with age, reaching its maximum value during the third decade of life, when fertility is at its peak. The observation that this ratio reaches 1.618 during this period, coinciding with the functional peak of the reproductive system, supports the idea that the golden ratio may serve as an indicator of biological optimization in living systems (Verguts *et al*., 2013). The heart, functioning in a highly synchronized and orderly manner within the human body, has increasingly become a subject of research from the perspective of the golden ratio (Yetkin *et al*., 2013; Yetkin *et al*., 2014; Papaioannou *et al*., 2019). In a study conducted on healthy individuals with physiological electrocardiography data, the average diastole-to-systole ratio was found to be 1.61, while the cardiac cycle to diastole ratio was 1.62. These findings suggest that the rhythmic pattern of the heart muscle closely aligns with the golden ratio and indicate its potential utility as a diagnostic parameter in identifying certain pathological conditions (Yetkin *et al*., 2013). In another study on the pulmonary system, it was reported that in individuals with pulmonary arterial hypertension and in the control group, fluctuations in systolic and diastolic pulmonary artery pressure exhibited a constant scaling factor corresponding to the golden ratio around the mean pulmonary artery pressure. This remarkable characteristic provides a new perspective that could enable the examination of pulmonary hemodynamic processes within the context of the golden ratio (Chemla *et al*., 2019). The golden ratio is not limited to the cardiovascular and pulmonary systems but has also been the subject of various studies in the auditory and craniofacial systems. The cochlea has drawn attention due to its spiral bony canal formation around the conical modiolus, resembling spiral structures in nature. Research has shown that the spiral structure of the cochlea aligns with the golden ratio, which optimizes sound perception efficiency and frequency tuning (Marinkovic *et al*., 2012). A study on craniofacial ratios found that the ratio of the distance between the anterior nasal spine and the nasion to the height of the piriform aperture falls within the golden ratio range in male individuals (Sertel Meyvaci *et al*., 2019). Moreover, Sarode *et al*. (2020), discovered that the oblique ridges of maxillary first molars and the triangular ridges of maxillary and mandibular premolars are divided into two segments following the golden ratio at the transverse and central grooves, respectively. The functional perfection of the occlusal table's strength and stability in posterior teeth has been attributed to the golden ratio. These findings provide new insights into the alignment of human facial proportions with the golden ratio.

In the present study, 57 ratios derived from different anatomical landmarks of the atlas were evaluated in relation to the golden ratio, considering its unique structure and critical role in the human body. The golden ratio was observed only in the P9/P22 ($p = 0.410$) and P18/P14 ($p = 0.159$) ratios. Nevertheless, the P1/P2, P1/P15, P9/P21, P10/P22, P12/P22, P18/P13, and P18/P20 ratios were also found to approximate the value of 1.618. These findings indicate that certain morphometric relationships within the atlas demonstrate a pattern consistent with the golden ratio, suggesting the presence of a distinctive geometric organization underlying its structural architecture. Evaluation of the ratios within the ± 0.5 SD interval revealed that 23 measurements clustered around the golden ratio. These ratios included P1/P2, P1/P15, P9/P21, P10/P21, P10/P22, P11/P21, P11/P22, P12/P21, P12/P22, P13/P21, P14/P21, P16/P9, P16/P10, P16/P12, P16/P13, P16/P14, P16/P20, P18/P13, P18/P20, P19/P21, P19/P12, and P20/P21. Furthermore, the notably high frequency values observed for the P18/P10, P18/P12, and P20/P22 ratios indicate that the proportional harmony of the atlas may not be limited to a few isolated measurements but may instead reflect a broader anatomical pattern.

In addition, comparison of atlas ratios according to sex revealed statistically significant differences in P1/P15, P1/P17, P4/P18, P7/P19, P8/P14, P8/P19, P16/P20, and P18/P19 ($p < 0.05$), suggesting that certain proportional relationships of the atlas may vary between male and female individuals.

Overall, although exact conformity to the golden ratio was observed in a limited number of ratios, the presence of numerous atlas ratios closely approximating 1.618 highlights the distinctive proportional organization of the atlas. These findings support the presence of a degree of aesthetic harmony and geometric order within the morphological architecture of the atlas, while also suggesting an underlying structural integrity that may be associated with the biomechanical and functional characteristics of the craniovertebral junction. Furthermore, the present study provides valuable morphometric reference data and offers new insights into the anatomical architecture of the atlas, thereby contributing to a deeper understanding of this unique vertebral structure.

## CONCLUSION

In conclusion, the present study provides valuable data on the evaluation of the atlas in terms of the golden ratio in the Turkish population. The aesthetic appearance of the atlas, which is noticeable to the naked eye, is further supported by the proximity of many of its ratios to the golden ratio. With these characteristics, the atlas plays a crucial role in the functional anatomy of the neck, serving as the primary structure that connects the head to the vertebra and facilitating mobility and cervical movements.

---

**MEYVACI, S. S.; ANKARALI, H.; BULUT, D. G.; CELIK, B. & TASKIN, B.** Evaluación de la proporción áurea en el atlas y sus características anatómicas únicas. *Int. J. Morphol., 44(3)*:959-967, 2026.

**RESUMEN:** Este estudio tuvo como objetivo evaluar si ciertas proporciones morfométricas del atlas se ajustan a la proporción áurea mediante el análisis de puntos de referencia anatómicos y parámetros específicos de su morfología única. Se analizaron imágenes de tomografía computarizada de haz cónico de 359 individuos (180 hombres, 179 mujeres), de 18 a 82 años de edad, para evaluar los parámetros morfométricos del atlas. Se midieron 22 parámetros morfométricos del atlas y se calcularon 57 proporciones a partir de estas mediciones. Con base en el valor medio de cada proporción evaluada y la desviación estándar (DE) correspondiente, los casos se clasificaron en cuatro grupos. Se determinaron las estadísticas descriptivas de las mediciones y las proporciones calculadas, incluyendo la media, la DE, la mediana, los percentiles 25 y 75, el recuento y las frecuencias porcentuales. La desviación de las proporciones calculadas con respecto a la proporción áurea se examinó mediante una prueba t de una muestra. Entre las 57 proporciones calculadas, la proporción áurea se observó solo en P9/P22 ($p = 0{,}410$) y P18/P14 ($p = 0{,}159$). Varias otras proporciones tuvieron valores medios cercanos a 1,618, incluyendo P1/P2 (1,697 ± 0,103), P1/P15 (1,664 ± 0,120), P9/P21 (1,685 ± 0,320), P10/P22 (1,691 ± 0,418), P12/P22 (1,691 ± 0,418), P18/P13 (1,661 ± 0,284) y P18/P20 (1,695 ± 0,401); sin embargo, estas proporciones difirieron significativamente de la proporción áurea. Los hallazgos proporcionan información valiosa sobre la relación entre las proporciones morfométricas del atlas y la proporción áurea en esta muestra de población turca. Se observó que varias proporciones eran numéricamente cercanas a la proporción áurea. Estos resultados proporcionan datos de referencia sobre la morfometría del atlas y sugieren que ciertas relaciones proporcionales del atlas pueden reflejar su organización anatómica distintiva.

**PALABRAS CLAVE: Morfometría del atlas; Serie de Fibonacci; Proporción áurea; Simetría; Población turca.**

**Author Contributions:** SSM: project development, literature review, manuscript writing, design and planning of the method; HA: project development, data analysis, manuscript editing, design and planning of the method; DGB: literature review, manuscript writing, design and planning of the method; BC: literature review, manuscript writing, critical revision of the text, editing of the text; BT: data collection, literature review, manuscript writing.

**Conflict of Interest:** There is no conflict of interest among the authors regarding the publication of this manuscript.

**Ethical Approval:** Ethical approval was received from Bolu Abant Izzet Baysal University, Non-Interventional Clinical Researches Ethics Committee Approval for the present study with decision number: 2024/382.

## REFERENCES

Bashour, M. An objective system for measuring facial attractiveness. *Plast. Reconstr. Surg., 118(3)*:757-74, 2006.

Benavoli, A.; Chisci, L. & Farina, A. Fibonacci sequence, golden section, Kalman filter and optimal control. *Signal Process., 89(8)*:1483-8, 2009.

Chemla, D.; Boulate, D.; Weatherald, J.; Lau, E. M. T.; Attal, P.; Savale, L.; Montani, D.; Fadel, E.; Mercier, O.; Sitbon, O.; Humbert, M. & Hervé, P. Golden ratio and the proportionality between pulmonary pressure components in pulmonary arterial hypertension. *Chest, 155(5)*:991-8, 2019.

Henein, M. Y.; Zhao, Y.; Nicoll, R.; Sun, L.; Khir, A. W.; Franklin, K. & Lindqvist, P. The human heart: application of the golden ratio and angle. *Int. J. Cardiol., 150(3)*:239-42, 2011.

Iosa, M.; Fusco, A.; Marchetti, F.; Morone, G.; Caltagirone, C.; Paolucci, S. & Peppe, A. The golden ratio of gait harmony: repetitive proportions of repetitive gait phases. *Biomed Res. Int., 2013*:918642, 2013.

Iosa, M.; Morone, G.; Bini, F.; Fusco, A.; Paolucci, S. & Marinozzi, F. The connection between anthropometry and gait harmony unveiled through the lens of the golden ratio. *Neurosci. Lett., 612*:138-44, 2016.

Kim, Y. H. Easy facial analysis using the facial golden mask. *J. Craniofac. Surg., 18(3)*:643-9, 2007.

Kolenkiewicz, M.; Wlodarczyk, A. & Wojtkiewicz, J. Diagnosis and incidence of spondylosis and cervical disc disorders in the University Clinical Hospital in Olsztyn, in years 2011-2015. *Biomed Res. Int., 2018*:5643839, 2018.

Lipiec, K.; Ryniewicz, W. I.; Groch, M.; Wieczorek, A. & Loster, J. E. The evaluation of anthropometric measurements of young Polish women's faces. *J. Craniofac. Surg., 30(3)*:709-12, 2019.

Mahakul, D. J. & Agarwal, J. Pentagon inside the circle of Willis and the golden ratio. *World Neurosurg., 156*:23-6, 2021.

Marinkovic, S.; Stankovic, P.; Strbac, M.; Tomic, I. & Cetkovic, M. Cochlea and other spiral forms in nature and art. *Am. J. Otolaryngol., 33(1)*:80-7, 2012.

Sanabria Medina, C.; Polo, L. C. & Botella, M. C. Dimorfismo sexual en primera vértebra cervical en una muestra de población colombiana. *Rev. Esp. Med. Leg., 37(4)*:140-5, 2011.

Padovan, L.; Ulbricht, V.; Groppo, F. C.; Neto, J. S. P.; Andrade, V. M. & Júnior, L. F. Sexual dimorphism through the study of atlas vertebra in the Brazilian population. *J. Forensic Dent. Sci., 11(3)*:158-62, 2019.

Papaioannou, T. G.; Vavuranakis, M.; Gialafos, E. J.; Karamanou, M.; Tsoucalas, G.; Vrachatis, D. A.; Soulis, D.; Manolesou, D.; Stefanadis, C. & Tousoulis, D. Blood pressure deviation from the golden ratio f and all-cause mortality: a Pythagorean view of the arterial pulse. *Int. J. Appl. Basic Med. Res., 9(1)*:55-7, 2019.

Park, A. E.; Fernandez, J. J.; Schmedders, K. & Cohen, M. S. The Fibonacci sequence: relationship to the human hand. *J. Hand Surg. Am., 28(1)*:157-60, 2003.

Purnell, M. C.; Butawan, M. B. A. & Ramsey, R. D. Bio-field array: a dielectrophoretic electromagnetic toroidal excitation to restore and maintain the golden ratio in human erythrocytes. *Physiol. Rep., 6(11)*:e13722, 2018.

Raposio, E.; Brocca, S. & Raposio, G. Relationship between the ideal female buttock and the golden ratio. *Plast. Reconstr. Surg. Glob. Open, 12(9)*:e6183, 2024.

Sarode, S. C.; Maniyar, N.; Sarode, G. S.; Yerwadekar, S.; Shetty, R.; Gadbail, A. R.; Gondivkar, S.; Anand, R. & Patil, S. Transverse ridge of premolars and oblique ridge of maxillary molars are in divine golden ratio. *J. Contemp. Dent. Pract., 21(5)*:486-9, 2020.

Sertel Meyvaci, S.; Hızal, M. & Ankaralı, H. Examination of craniofacial parameters in Turkish males with golden ratio in piriform aperture size. *J. Surg. Med., 5(3)*:289-93, 2021.

Sertel Meyvaci, S.; Ankarali, H.; Bulut, D. G. & Taskin, B. Performances of different classification algorithms in sex determination from first cervical vertebra measurements. *Int. J. Morphol., 42(5)*:1439-46, 2024.

Sertel Meyvaci, S.; Arifoglu, Y.; Gurel, S. & Buber, A. Radio-anatomical examination from foramen transversarium of first cervical vertebra for sex estimation. *Forensic Sci. Int. Rep., 2*:100078, 2020.

Sertel Meyvaci, S.; Kosif, R.; Bamaç, B.; Hizal, M. & Ankarali, H. Evaluation of apertura piriformis and related cranial anatomical structures through computed tomography: golden ratio. *Folia Morphol., 78(4)*:839-46, 2019.

Stakhov, A. & Sluchenkova, A. *A museum dedicated to the concept of harmony and the golden section*. In R. Sarhangi (Ed.), Bridges: Mathematical connections in art, music, and science. 2002. pp. 269–76. Bridges Conference.

Verguts, J.; Ameye, L.; Bourne, T. & Timmerman, D. Normative data for uterine size according to age and gravidity and possible role of the classical golden ratio. *Ultrasound Obstet. Gynecol., 42(6)*:713-7, 2013.

Walker, F. D.; Kubba, H. & Clement, W. A. Use of facial proportions in pinnaplasty assessment. J. Plast. Reconstr. Aesthet. Surg., 64(8):1110-3, 2011.

Yamagishi, M. E. & Shimabukuro, A. I. Nucleotide frequencies in human genome and Fibonacci numbers. *Bull. Math. Biol., 70(3)*:643-53, 2008.

Yetkin, E.; Topbas, U.; Yanik, A. & Yetkin, G. Does systolic and diastolic blood pressure follow golden ratio? *Int. J. Cardiol., 176(3)*:1457-9, 2014.

Yetkin, G.; Sivri, N.; Yalta, K. & Yetkin, E. Golden ratio is beating in our heart. *Int. J. Cardiol., 168(5)*:4926-7, 2013.

Corresponding Author:
Beyza Celik
Department of Anatomy
Faculty of Medicine
Bolu Abant Izzet Baysal University
Bolu
TURKIYE

E-mail: beyzayilmazcelik1@gmail.com
0000-0003-4401-8678 beyzayilmazcelik1@gmail.com

**Seda Sertel Meyvaci:**
0000-0002-9450-145X sedasertelmeyvaci@gmail.com
**Handan Ankarali:**
0000-0002-3613-0523 handanankarali@gmail.com
**Duygu Goller Bulut:**
0000-0003-4260-2520 duygugoller@hotmail.com
**Betul Taskin:**
0000-0002-8270-6634 betul.taskin@ibu.edu.tr